Clim Dyn (2009) 33:245–263
DOI 10.1007/s00382-008-0511-6

Indian Ocean sea surface salinity variations in a coupled model

P. N. Vinayachandran · Ravi S. Nanjundiah

Received: 14 February 2008 / Accepted: 12 December 2008 / Published online: 25 January 2009

Abstract The variability of the sea surface salinity (SSS) in the Indian Ocean is studied using a 100-year control simulation of the Community Climate System Model (CCSM 2.0). The monsoon-driven seasonal SSS pattern in the Indian Ocean, marked by low salinity in the east and high salinity in the west, is captured by the model. The model overestimates runoff into the Bay of Bengal due to higher rainfall over the Himalayan–Tibetan regions which drain into the Bay of Bengal through Ganga–Brahmaputra rivers. The outflow of low-salinity water from the Bay of Bengal is too strong in the model. Consequently, the model Indian Ocean SSS is about 1 less than that seen in the climatology. The seasonal Indian Ocean salt balance obtained from the model is consistent with the analysis from climatological data sets. During summer, the large freshwater input into the Bay of Bengal and its redistribution decide the spatial pattern of salinity tendency. During winter, horizontal advection is the dominant contributor to the tendency term. The interannual variability of the SSS in the Indian Ocean is about five times larger than that in coupled model simulations of the North Atlantic Ocean. Regions of large interannual standard deviations are located near river mouths in the Bay of Bengal and in the eastern equatorial Indian Ocean. Both freshwater input into the ocean and advection of this anomalous flux are responsible for the generation of these anomalies. The model simulates 20 significant Indian Ocean Dipole (IOD) events and during IOD years large salinity anomalies appear in the equatorial Indian Ocean. The anomalies exist as two zonal bands: negative salinity anomalies to the north of the equator and positive to the south. The SSS anomalies for the years in which IOD is not present and for ENSO years are much weaker than during IOD years. Significant interannual SSS anomalies appear in the Indian Ocean only during IOD years.

Keywords Indian Ocean · Salinity · Interannual variation · Coupled model · Indian Ocean Dipole

P. N. Vinayachandran (✉) · R. S. Nanjundiah
Centre for Atmospheric and Oceanic Sciences,
Indian Institute of Science, Bangalore 560 012, India
e-mail: vinay@caos.iisc.ernet.in

1 Introduction

Vertical stratification in the ocean is dependent on salinity and therefore salinity plays an important role in the near-surface thermodynamics of tropical oceans (Miller 1976; Cooper 1988; Lukas and Lindstrom 1991; Sprintall and Tomczak 1992; Murtugudde and Busalacchi 1998). Reduction of sea surface salinity as a result of rainfall or river discharge into the ocean can lead to the formation of a barrier layer, which may prevent entrainment of cooler thermocline water into the mixed layer and consequently maintain warmer sea surface temperature. The penetration of solar radiation below the mixed layer (which is found to be thin in regions of low salinity) can lead to the formation of sub-surface temperature inversions in the ocean (Anderson et al. 1996; Kurian and Vinayachandran 2006). Salinity effects have been found to influence the mixed layer depth in several places in the tropical ocean (Sprintall and Tomczak 1992; Murtugudde and Busalacchi 1998). In the Indian Ocean, a barrier layer has been observed in the Bay of Bengal (Vinayachandran et al. 2002a), eastern equatorial Indian Ocean (Eriksen 1979; Godfrey et al. 1999) and in the southeastern Arabian Sea (Shankar et al. 2004). Salinity effects can also lead to dynamic height

variations and changes in velocity by affecting the momentum distribution (Han et al. 1999; Howden and Murtugudde 2001).

The sea surface salinity (SSS) distribution in the North Indian Ocean exhibits large spatial variability (Donguy and Meyers 1996). The Arabian Sea is characterized by high salinities due to the excess of evaporation over precipitation (Rao and Sivakumar 2002) and its proximity to two high-salinity seas namely, the Red Sea and the Persian Gulf. On the other hand, the Bay of Bengal has large excess of precipitation over evaporation and is a receptor of large discharge from several rivers. Consequently, the salinity in the Bay of Bengal is much below the mean salinity of the world oceans. The high rainfall received in the eastern equatorial Indian Ocean causes the salinity there to be less than that in the west. Thus, in general, the eastern half of the Indian Ocean has lower salinity than the west.

The seasonal salinity balance in the Indian Ocean is determined by the fresh water sources/sinks and the redistribution of the resulting low/high-salinity water by ocean currents (Rao and Sivakumar 2002). The seasonally reversing monsoon currents in the North Indian Ocean (Schott and McCreary 2001; Shankar et al. 2002) transport low and high-salinity waters from their source regions and the horizontal SSS patterns are strongly influenced by ocean circulation. Within the Bay of Bengal, the East India Coastal Current (EICC) and the North Bay Monsoon Current export fresh water away from the source region (Shetye et al. 1991; Vinayachandran et al. 2002b; Vinayachandran and Kurian 2007). The EICC (Shetye et al. 1996) carries low-salinity water from the river mouths into the southern Bay of Bengal (Vinayachandran et al. 2005) and into the eastern Arabian Sea (Shetye et al. 1991; Shenoi et al. 2005; Kurian and Vinayachandran 2007; Durnad et al. 2007). In addition, a substantial amount of low-salinity water escapes from the Bay of Bengal along the eastern boundary (Han and McCreary 2001; Howden and Murtugudde 2001; Jensen 2001, 2003; Sengupta et al. 2006). The seasonally reversing monsoon currents (Shankar et al. 2002) facilitate exchange of water between the Arabian Sea and the Bay of Bengal. During winter, cool northeasterlies blowing over the northern Arabian Sea (McCreary et al. 1993) lead to the formation of a high-salinity water mass (Shenoi et al. 1993), which advects southward along with the monsoon currents. During summer, the Southwest Monsoon Current carries high-salinity Arabian Sea water into the Bay of Bengal (Vinayachandran et al. 1999a). Elsewhere, in the equatorial Indian Ocean, the Wyrtki jets affect the distribution of low-salinity water in the eastern equatorial Indian Ocean (Masson et al. 2002) and the Somali Current in the western Arabian Sea transports low-salinity water northward (Schott and McCreary 2001).

Owing to the paucity of data, little is known about the interannual variability of SSS in the North Indian Ocean. Nevertheless, limited amount of repeat observations that are confined to shipping lanes suggest that salinity variability could be high in the tropical Indian Ocean (Delcorix et al. 2005). Rao and Sivakumar (2002) also found from SSS data along two shipping lanes that considerable interannual variability occurs during El Nino years. Large interannual freshening anomalies occur in the Indo-Australian basin due to advection of freshwater from the Indonesian Seas (Phillips et al. 2005). Salinity anomalies in the eastern equatorial Indian Ocean feed-back onto the sea surface temperature anomalies. Masson et al. (2004) found that salinity effects reinforced oceanic anomalies and enhanced air–sea interaction favourable for the evolution of the 1997 Indian Ocean Dipole (IOD). In the Bay of Bengal, however, interannual sea level variations are not affected by the interannual variations of river discharge (Han and Webster 2002). Barring the few studies (such as the ones listed above), however, details of basin-wide spatio-temporal structure of the interannual variations of Indian Ocean SSS and their mechanisms have not yet been pursued.

A major hurdle for interannual salinity simulation by ocean models is the lack of reliable freshwater forcing. Reliable estimate of one of its components, namely rainfall, has recently become available from different sources. Among different precipitation products, CMAP (Climate Prediction Centre Merged Analysis of Precipitation; Xie and Arkin 1998) data set produces salinity simulation closest to the observation (Yu and McCreary 2004). Thus, in the eastern equatorial Indian Ocean where interannual SSS anomalies are caused by precipitation anomalies and ocean dynamics (Perigaud et al. 2003), interannual simulation of salinity have been possible. However, there are no reliable interannual estimates of runoff that can be used for forcing ocean models. Estimation of river discharge by the inversion of ocean model simulation (Yaremchuk et al. 2005) appears to be promising but this has not been attempted at interannual time scale.

Coupled models have the advantage that forcing for the ocean is obtained from component models of atmosphere and land and no external forcing data sets are necessary. Coupled models have been used for studying the interannual variations of salinity in the Pacific and Atlantic Oceans (e.g. Mignot and Frankignoul 2003), but no such study has been reported for the Indian Ocean. Coupled model studies concerning the Indian Ocean have focused on air–sea interaction, particularly in association with the IOD (Iizuka et al. 2000; Gualdi et al. 2003; Lau and Nath 2003). In this paper, we investigate the Indian Ocean SSS variability using the output from a coupled model that is described in Sect. 2. We first examine the seasonal salinity

variations and associated processes and compare them with climatologies and existing analyses (Sect. 3). We then examine the interannual variability (Sect. 4) and show that significant salinity variability occurs in the North Indian Ocean only during the IOD years (Sect. 5). Important results from this study are summarised in Sect. 6.

2 The coupled model

The model used in this study is the Community Climate System Model version 2 (CCSM2) which consists of an atmospheric model, an ocean model, a land–surface model and a sea–ice model (Kiehl and Gent 2004). The individual models interact through a coupler. The atmospheric model, the Community Atmospheric Model (CAM2), was run at T-42 resolution, i.e. a resolution of about 280 km and with 26 vertical levels. We have used Eulerian dynamics with semi-Lagrangian moisture transport for our simulation. The parameterization of cumulus convection is done using the Zhang and McFarlane (1995) scheme. Shortwave computations are done using the method of Briegleb (1992). The land model used in the present study was the Community Land Model version 2.0 (CLM2.0) at T-42 resolution (i.e. same as that of the atmosphere). CLM2 (Bonan et al. 2002) has a river runoff scheme to route stream flows.

The ocean model used in CCSM2 is the Parallel Ocean Program (POP), which interacts with the atmospheric model through the coupler, once a day. The longitudinal resolution in the model is approximately 1° whereas the grid spacing is variable in the meridional direction. It is 0.27° at the equator, decreasing to 0.54° at 33° and remaining at this value at higher latitudes. The model has 40 vertical levels, the thickness of which varies from 10 m in the top 50–250 m in the deep ocean. The horizontal mixing scheme in the model uses spatially dependent meridional and zonal viscosity coefficients (Smith and McWillimas 2003; Smagorinsky 1963) and the K-profile parameterization (Large et al. 1994) is used for vertical mixing. Further details of the ocean model as well as other component models may be found in Smith and Gent (2002). A spin-up initial condition, at the end of a 350-year integration was obtained from NCAR and the model was integrated for 100 years starting from this initial condition. Details of the experiment and initial model evaluation have been presented in Janakiraman et al. (2005)

Janakiraman et al. (2005) compared the mean monsoon rainfall and its interannual variability in this simulation with observations and found that the coupled model offers significant improvement in rainfall simulation because the coupled evolution of monsoon is represented better in the coupled model (Nanjundiah et al. 2005). Consequently, the CCSM simulation is able to capture the high rainfall over the Bay of Bengal. This is crucial for this study because, as we shall show, fresh water input into the Bay of Bengal is a focal point that determines the interannual SSS variability of a much larger region in the Indian Ocean. The model interannual variability of the Indian summer monsoon rainfall is much larger compared to observations. However, a typical character of this interannual variability is that years of high rainfall is interspersed with that of low variability and this feature is well captured by the model. The model also reproduces the seasonal cycle of sea surface temperature in the Indian Ocean, but the simulated temperature is slightly cooler compared to climatology. For a detailed description of the model please see Janakiraman et al. (2005).

3 Seasonal climatology

3.1 Salinity

Figure 1 compares the seasonal cycle of SSS in the Indian Ocean simulated by the CCSM2 with the World Ocean Atlas 2001 (WOA2001) climatology (Conkright et al. 2002). In the north Indian Ocean, the western part has higher salinity and the eastern part shows lower salinity due to the asymmetry in the fresh water forcing which is marked by large excess in the Bay of Bengal and deficit in the Arabian Sea (Donguy and Meyers 1996; Boyer and Levitus 2002; Rao and Sivakumar 2002). The high-salinity water in the Arabian Sea spreads southward and into the Bay of Bengal during the summer monsoon (Murty et al. 1992; Vinayachandran et al. 1999a). Also, the low-salinity water flows out of the Bay of Bengal along its eastern boundary (Shetye et al. 1996; Han and McCreary 2001; Jensen 2001; Sengupta et al. 2006). This seasonal sloshing and spreading of low and high-salinity water is simulated by the CCSM (Fig. 1).

The northern Bay of Bengal is the major source region for low-salinity water in the Indian Ocean. Large differences between the model salinity and climatology are seen in this region (Fig. 1). The model salinity in the northern Bay of Bengal near the river mouths is less than that of the climatology throughout the year. Spreading of the river plume along the coasts during the peak summer monsoon months, however, is similar between the model and data. The transport of low-salinity water by the EICC (Shetye et al. 1996) during the winter is clearly seen in the model simulation (Fig. 1). Part of this low-salinity water is also seen to reach the southeastern Arabian Sea during the winter monsoon, consistent with the climatology. The equatorial Indian Ocean shows higher salinity in the west and lower salinity in the east in both observations and

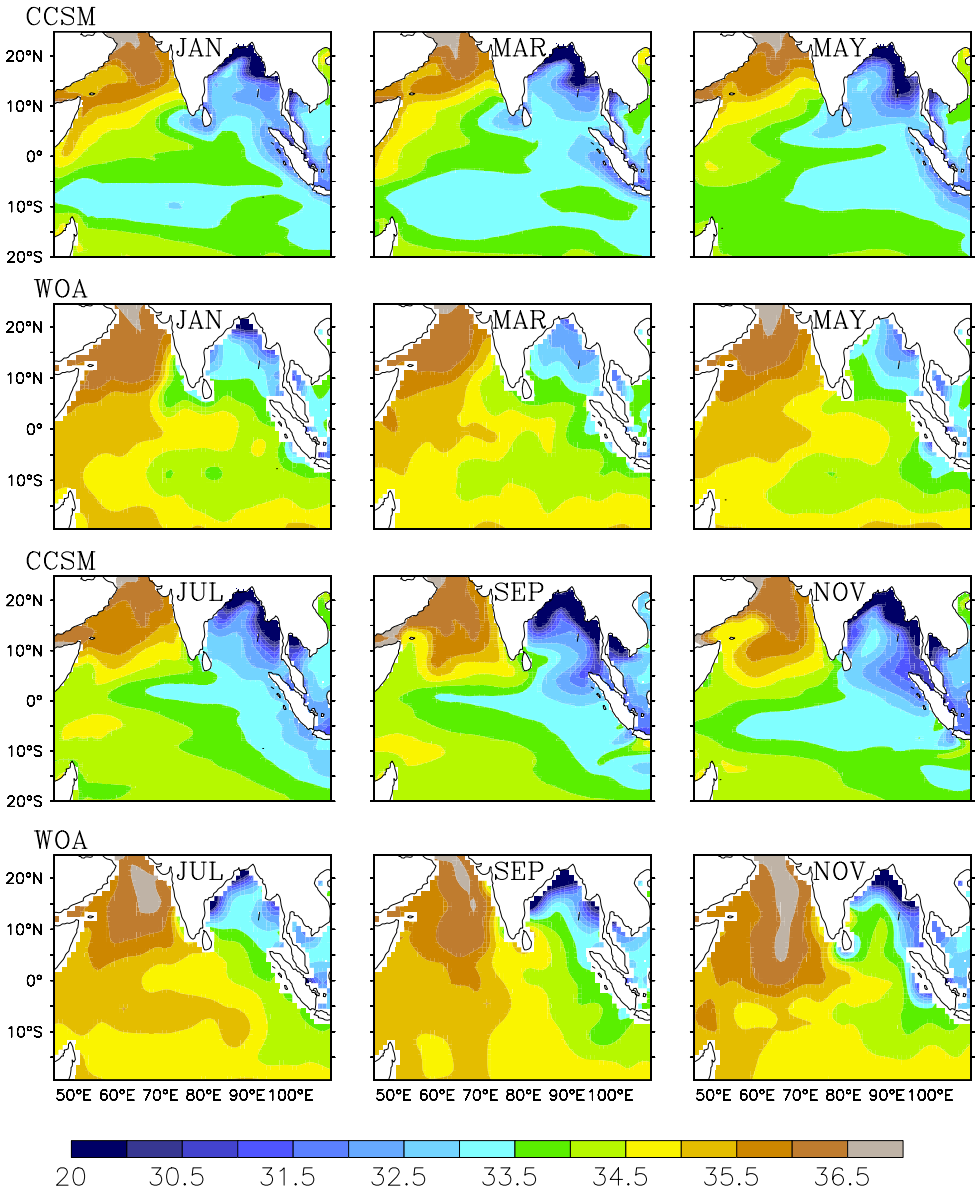

Fig. 1 Bimonthly maps of sea surface salinity (SSS) in the Indian Ocean from WOA01 Climatology (Conkright et al. 2002) and from CCSM2. *Rows 1* and *3* correspond to the model and *rows 2* and *4* to observations

simulations. The model salinities are, however, 1–1.5 less than the WOA01 climatology.

This difference between the model and climatology can be attributed to the Bay of Bengal being too fresh and advection of this fresh water. Although climatological data show low salinities near the river mouths during the pre-monsoon months of March–May, the model salinity in these regions is too low during these months (Fig. 1). The model salinity near the northern boundary of the bay during March is less than 25 whereas in the climatology it is above 30. Similar differences are also seen during the summer monsoon. In addition, the outflow of low-salinity water from the Bay of Bengal along its eastern boundary occurs too early in the model. These deficiencies in the model simulation are the reasons for the basin-wide decrease in salinity in the model.

On the whole, the major features of SSS and its seasonal cycle in the CCSM are similar to that in the climatology. However, the models SSS is too fresh over most of the Indian Ocean throughout the year. This difference is very high in the northern Bay of Bengal where there is large river runoff into the ocean.

3.2 Freshwater input

The flux of fresh water from the atmosphere as well as from the land affects the salinity distribution in the ocean. Therefore, it is essential that the model reproduce these forcing fields realistically in order to simulate the salinity field accurately. In this section, we compare the difference between evaporation and precipitation (E − P), runoff and their seasonal variations with observations. For observations

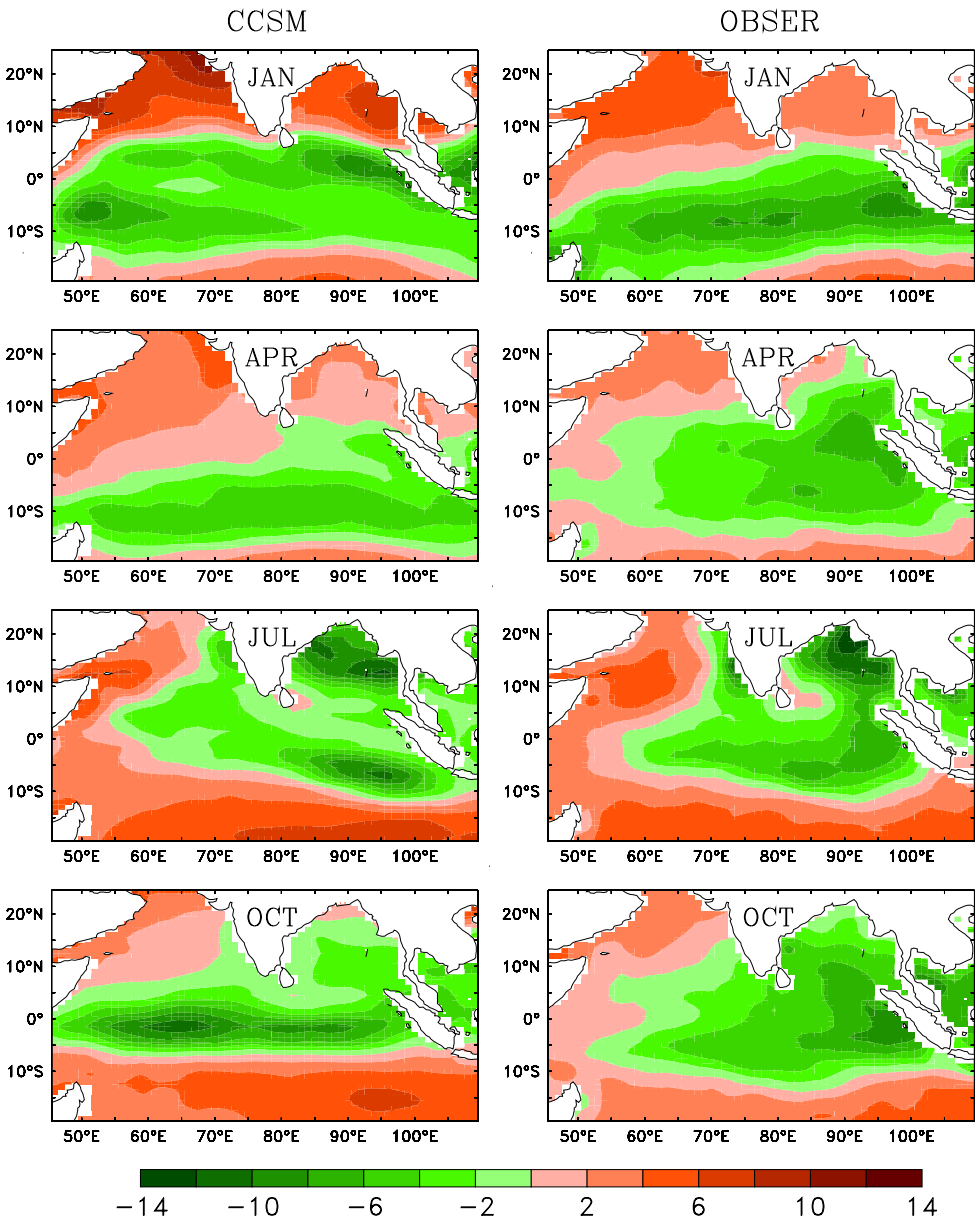

Fig. 2 E–P (mm/day) from the model (*left panels*) and from observed climatologies (*right panels*). For observation, evaporation is taken from Josey et al. (1999) and precipitation from CMAP (Xie and Arkin 1998). Positive values (*shaded in red*) indicate that evaporation exceeds precipitation

we use Josey et al. (1999) climatology for evaporation and CMAP (Xie and Arkin 1998) climatology for precipitation. The CMAP precipitation climatology used here is for the period January 1979–September 2004 and is obtained from http://www.cdc.noaa.gov/cdc/data.cmap.html.

The difference between evaporation and precipitation (E − P) is compared in Fig. 2 for January, April, July and October. The observed E–P climatology shows freshwater loss to the atmosphere to the north of about 5°N during December–April and gain to the south of it up to about 15°S. During the summer monsoon, the Bay of Bengal and the eastern Arabian Sea becomes regions of excess precipitation over evaporation; this pattern is present during May–October. This overall pattern is simulated well by the model but there are several differences between the model and climatology.

In January, there is a net gain of freshwater by the ocean from the atmosphere between about 15°S and 10°N and loss elsewhere. This gain in the observations has one maximum in the southern tropical Indian Ocean. The model, however, shows two regions of high values, one in the southern Bay of Bengal and the other between 0° and 10°S in the west. This difference is due to the deficiency in the simulation of the rainfall in the model; the model rainfall shows two highs compared to one seen in the CMAP data set. The loss of freshwater in the Arabian Sea and Bay of Bengal is overestimated in the model due to the lager evaporation in the model than in the observations.

Similar differences are also noted during April. In the model, there is a band of fresh water gain that stretches all across the Indian Ocean whereas the data show much larger meridional spread than in the model and the band weakens towards the west. During the summer monsoon, both model and observations show three regions of heavy rainfall; off the west coast of India, over the Bay of Bengal and in the eastern equatorial Indian Ocean. The model rainfall in the eastern equatorial Indian Ocean is stronger; in the Bay of Bengal, it is too far away from the coast, and in the Arabian Sea, it is weaker leading to magnitudes of the freshwater water flux differing from that in the observations, although the overall spatial pattern is similar in both observations and model.

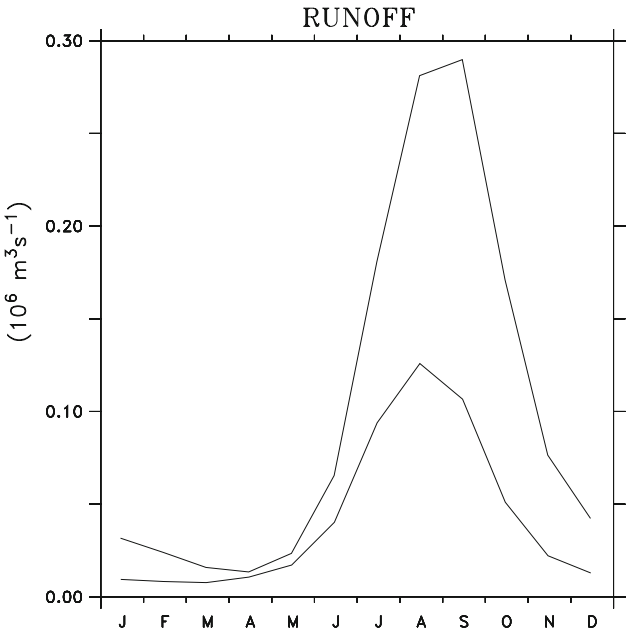

Fig. 3 Runoff from the model into the northern Bay of Bengal (*thick line*) compared to the observed climatological discharge (*thin line*). In the case of model, runoff into the Bay of Bengal to the north of 10°N is taken. Observations are from SAGE/UNESCO (Vorosmarty et al. 1996) and all rivers for which data is available are taken into account

There is large input of fresh water into the Bay of Bengal from runoff. Considering that this is a major forcing function for Indian Ocean salinity we have attempted to compare the runoff in the model with observations. This is not an easy task for several reasons. There are several major and minor rivers discharging into the Bay of Bengal. We have taken discharge data for all the rivers in the Bay of Bengal that are available from the Global River Discharge Database (http://www.sage.wisc.edu/riverdata; Vorosmarty et al. 1996). For model discharge we have integrated the runoff into the Bay of Bengal to the north of 10°N. The annual cycle of the runoff is similar in both model and observations (Fig. 3). However, the peak discharge in the model is much larger than in the data. Note that the actual river discharge into the Bay of Bengal can be larger than that seen in Fig. 3 because, often the discharge measurement stations are located upstream [whether the exclusion of Bangladesh discharge is causing this difference could not be confirmed using the model

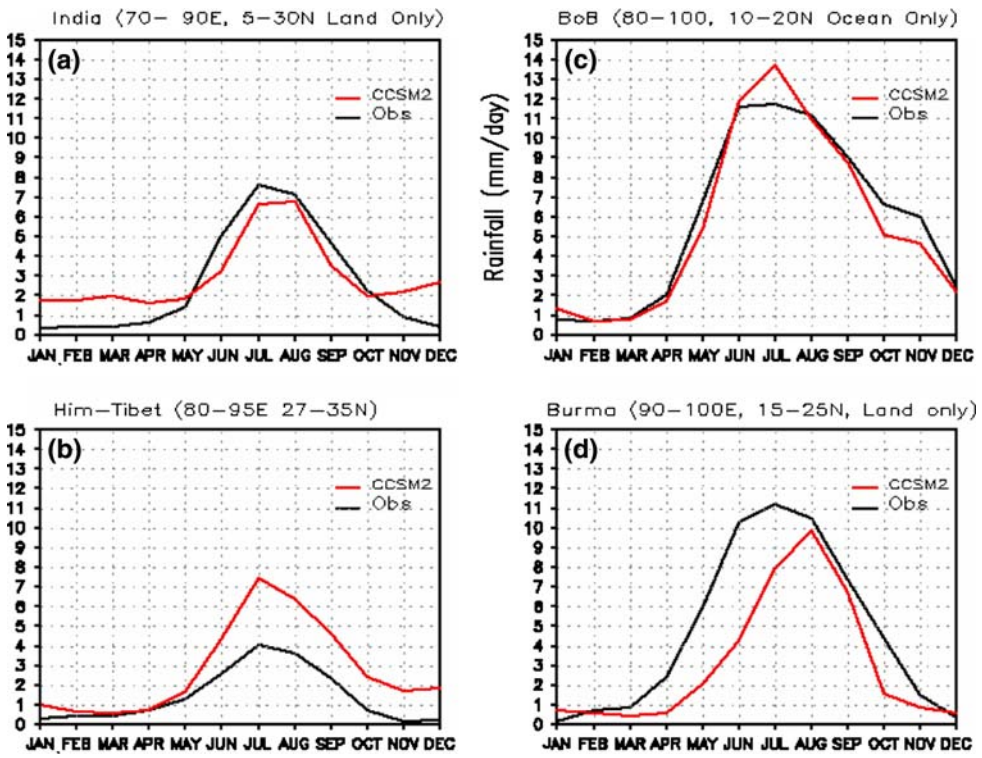

Fig. 4 Seasonal cycle of rainfall (mm/day) in observations and CCSM2 over **a** Indian region, **b** Himalayan and Tibet region, **c** Bay of Bengal and **d** Burmese region

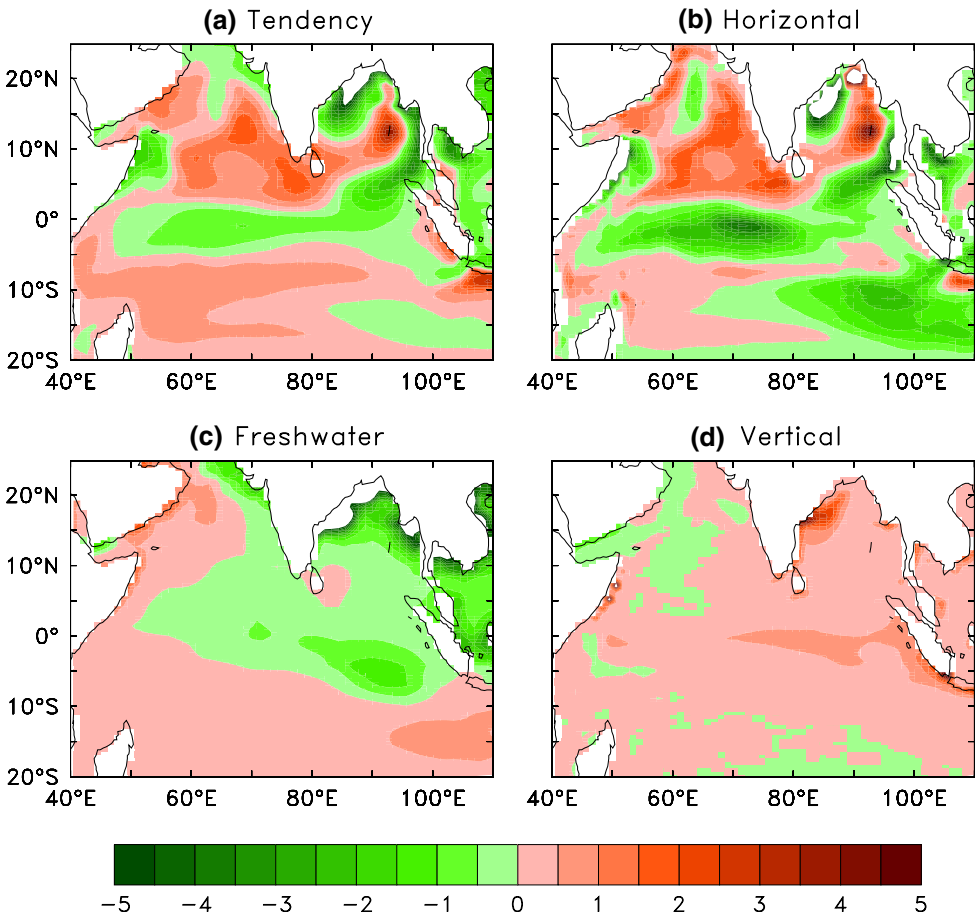

Fig. 5 Terms of the salinity equation for July. **a** Local rate of change of salinity, **b** contribution from horizontal advection, **c** contribution from fresh water input and **d** contribution from vertical processes. The *white patches* in the Bay of Bengal indicate values beyond the *color bar*. Units are $10^{-07}s^{-1}$

because (a) Bangladesh is represented by little more than one grid point in the model and (b) the model appears to underestimate the Bangladesh rainfall]. In addition, discharge data for rivers such as Irrawady, Meghna and Salween are not available. Nevertheless, considering that the difference between the model and data is huge and the simulated salinities are too low, it is reasonable to conclude that the model overestimates runoff into Bay of Bengal. We next examine the processes responsible for this high runoff.

3.3 Cause of high runoff

Since runoff is related to precipitation, we analyse the simulation of the seasonal cycle of rainfall over the Indian region. The seasonal cycle of rainfall over India simulated by CCSM2 (Fig. 4a, also shown by Nanjundiah et al. 2005) compares well with the observed seasonal cycle over this region. Therefore, the cause of the large runoff into the Bay of Bengal appears to be very intriguing. In addition to the Indian region, rainfall over the Tibetan plateau and the Burmese region contribute to runoff into the Bay of Bengal. The high runoff could be due to higher rainfall over these regions or due to problems with the runoff parameterization. The Himalayan–Tibetan region primarily drains into the Bay of Bengal by Brahmaputra and, to a lesser extent, by the Ganga river systems. The rainfall over this region is significantly overestimated by the model (Fig. 4b). This could be related to the steep orography over this region and to the interaction between orography and cumulus parameterization. The other region of significant orography is the Burmese coast adjoining the Bay of Bengal. Though these mountains are short and narrow, they play a significant role in enhancing rainfall over this region (Xie et al. 2006). High rainfall from this region drains into the Bay of Bengal primarily through the Irrawady and Salween river systems. Analysing the simulated rainfall over this region, we notice that the model consistently underestimates Burmese rainfall (Fig. 4d). This could be due to the coarse resolution of the atmosphere model because of which the narrow Burmese orography is not resolved. The resolution of this orography is extremely important for realistic simulation of high rainfall over the Burmese region.

Freshwater influx in the form of precipitation over the Bay of Bengal can also have a significant impact on salinity. Comparing the seasonal cycle of rainfall over Bay of Bengal (Fig. 4c), we notice that the local rainfall over the Bay is in close agreement with the observed. Only

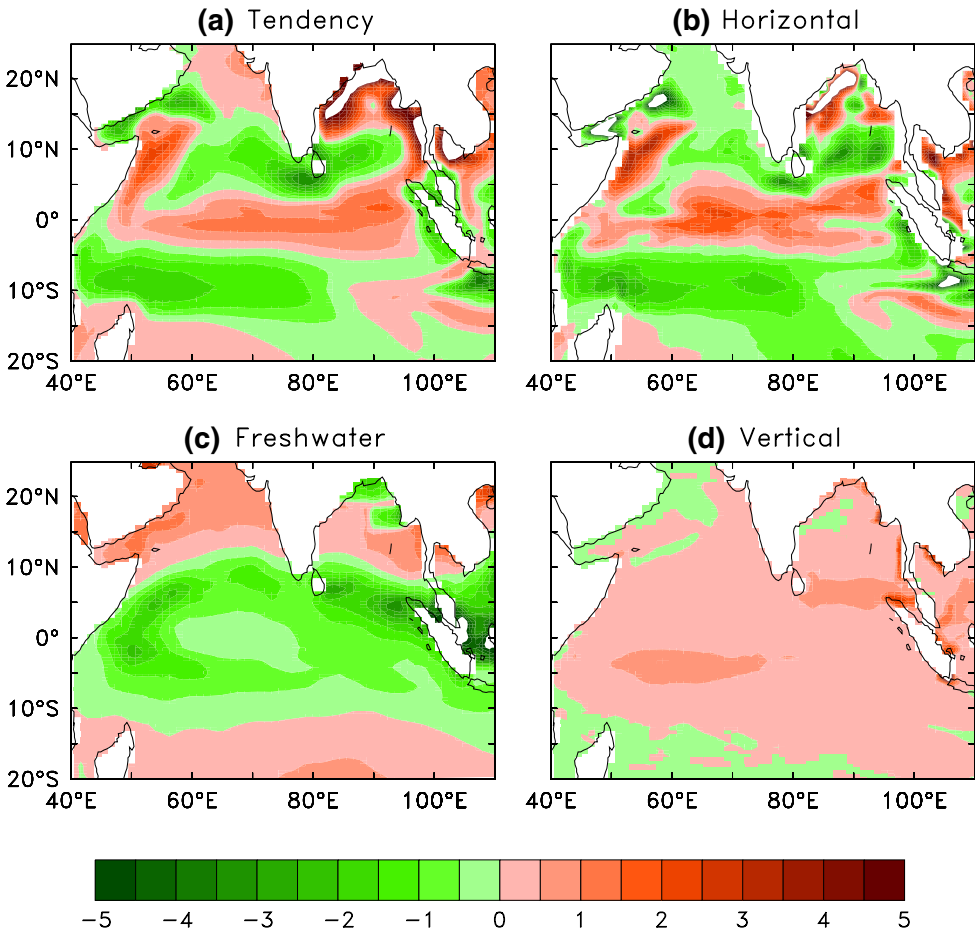

Fig. 6 Same as in Fig. 5 but for November

during the peak monsoon month of July does the model slightly overestimate the rainfall over this region. Thus, it appears that low salinity in model simulations is caused by higher runoff into the Bay and the overestimation of rainfall over the Himalayan and Tibetan region is the cause for this higher runoff.

3.4 Processes

The equation for the conservation of salt within the mixed layer (Ferry and Reverdin 2004), neglecting mixing and diffusion, can be written as

$$\partial S/\partial t = (-u\,\partial S/\partial x - v\,\partial S/\partial y) + ((S_{-h} - S)\Gamma(W_{-h})W_{-h} + (S - S_{-h})\mathrm{d}h/\mathrm{d}t)/h + (E - P - R)S/h \quad (1)$$

where S, u, and v are the mixed-layer salinity, zonal velocity and meridional velocity respectively, W_{-h} and S_{-h} are the vertical velocity and salinity respectively at the base of the mixed-layer, and Γ is a Heaviside step function depending on W_{-h}. E is evaporation, P is precipitation, and R is runoff, and their sum gives the net freshwater flux into the ocean. The first, second and third terms in the above equation represent the contribution from horizontal processes, vertical processes and freshwater input to the salinity tendency respectively (Ferry and Reverdin 2004).

Figure 5 shows the salinity balance for July. Large decrease in salinity is noticed in the western Bay of Bengal (Fig. 5a) due to the large freshwater input into this region from rivers as well as rainfall (Fig. 5c). The eastern boundary of the Bay of Bengal and parts of the EIO also show freshening. In the eastern Bay, this is attributed to fresh water flux and it southward advection. The freshening in the equatorial Indian Ocean is caused by the advection low-salinity water from the Bay of Bengal (Fig. 5b). Parts of central Bay and eastern Arabian Sea show increase in salinity due to the advection by monsoon currents (Murty et al. 1992; Vinayachandran et al. 1999a; Shankar et al. 2002). There is a non-trivial advection of low-salinity water through the Indonesian throughflow but this does not have a significant impact of the salinity change due to the opposing effect of freshwater input (Fig. 5c).

Vertical processes have significant contributions only in two regions; one in the western Bay of Bengal and the other off Sumatra. It is in these regions that the SSS shows very low values creating large vertical gradients and strong

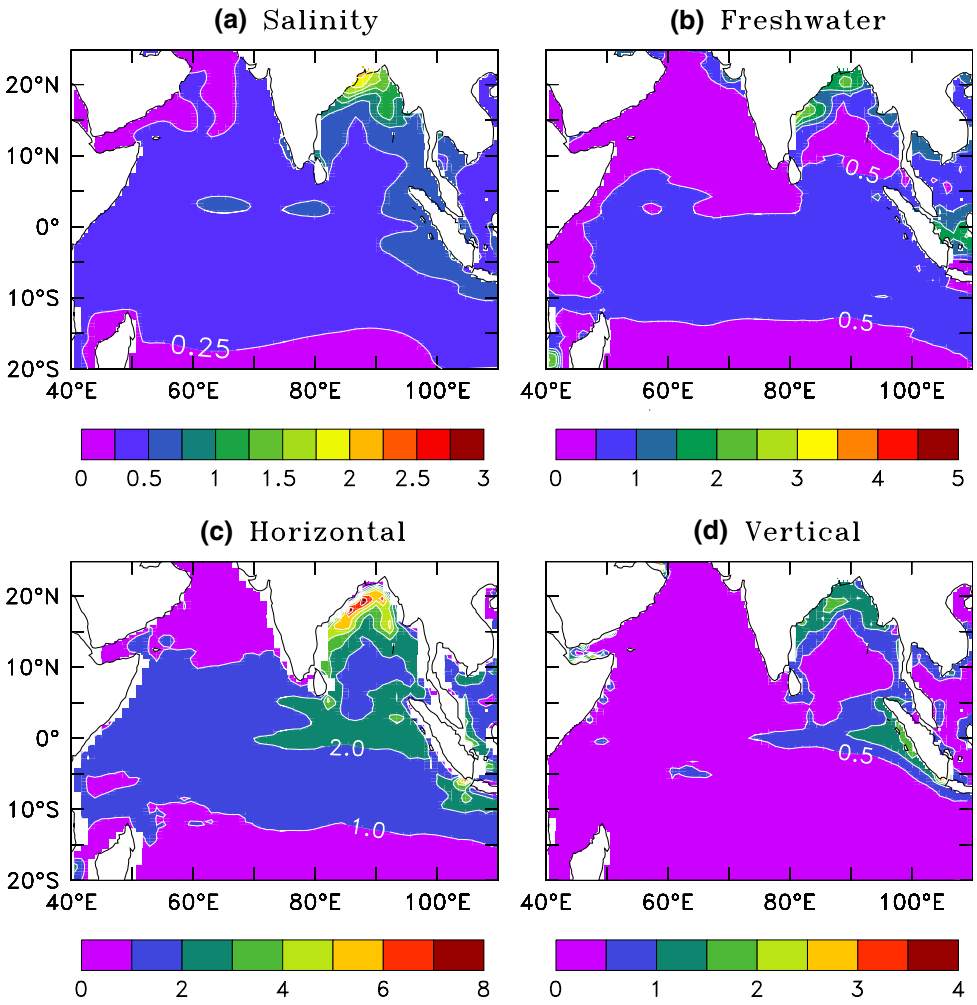

Fig. 7 Standard deviation of anomalies of (**a**) sea surface salinity (psu) (**b**) from freshwater input term (**c**) horizontal advection term and (**d**) vertical processes term from CCSM2 for the 100-year period. Units for salinity are psu and for the other three are 10^{-07} s^{-1}

stratified layer. Off the coast of Somalia, there is a decrease in salinity and an increase off the coast of Oman, associated with the monsoon circulation (Schott and McCreary 2001). In the Bay of Bengal, vertical processes have significant contribution around the confluence of the poleward flowing EICC and a freshwater plume that moves southward (Shetye et al. 1991). The EICC is driven by poleward alongshore winds and the latter by wind stress curl in the Bay of Bengal and remote forcing from the equatorial Indian Ocean (Shankar et al. 1996, McCreary et al. 1996; Vinayachandran et al. 1996). The fresh plume subducts below the EICC and flows as an undercurrent and during this process considerable vertical exchange of salt and freshwater takes place. The vertical exchange of salt taking place off Sumatra is attributed to coastal upwelling.

The pattern of local rate of change of SSS in November is very different from that in July (Fig. 6a). Salinity in the western Bay of Bengal increases in November due to the export of the low-salinity water by the EICC (Shetye et al. 1996). In fact, the entire coastal region of the Bay shows an increase as the freshwater received during the summer monsoon is removed by ocean circulation. Advective process (Fig. 6b) contribute to an increase in salinity along the coast and decrease in the southern parts of the Bay (Vinayachandran et al. 2005). The decrease in salinity in the southeastern Arabian Sea is also attributed to the advection by coastal currents and the Winter Monsoon Current. To the south of the Bay of Bengal, between 10°S and 10°N, there is high rainfall in the model, but the salinity tendency is dominated by horizontal advection. A similar process also occurs in the southwestern tropical Indian Ocean. In the western Arabian Sea, the opposing tendencies off the coast of Somalia and Oman are also determined by horizontal advection. In summary, the winter SSS distribution, in general, is determined by horizontal advection.

Rao and Sivakumar (2002) carried out a similar analysis using a climatological data set. They found that advection by ocean circulation determines the spatial distribution of salinity during winter. During summer, the large fresh water input into the Bay of Bengal and its redistribution stands out prominently in the spatial pattern. The results

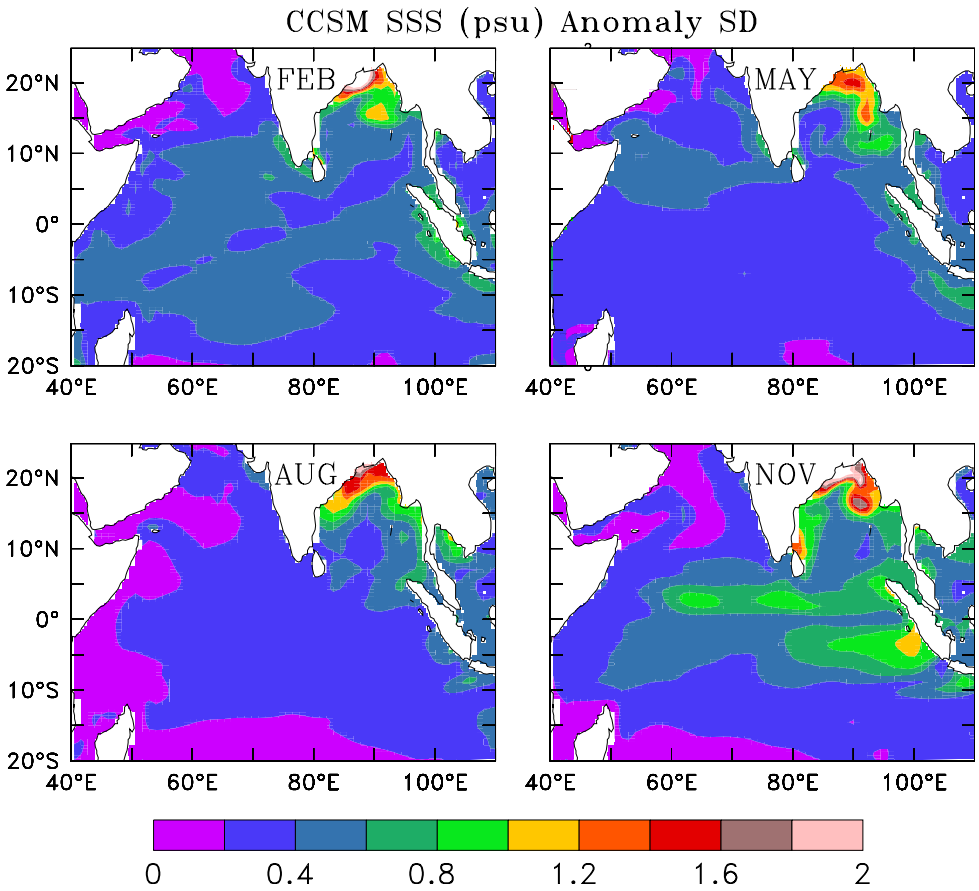

Fig. 8 Monthly standard deviations of sea surface salinity for February (*top left panel*), May (*top right panel*), August (*bottom left panel*) and November (*bottom right panel*)

obtained from the present analysis is very similar to that of Rao and Sivakumar (2002), suggesting that the CCSM2 has a realistic representation of the salt balance in the north Indian Ocean.

The large variability of freshwater input and its advection in the Bay of Bengal suggests two pathways for the export of freshwater from the Bay of Bengal. One is along the east coast of India and the other along the eastern boundary of the bay. The former takes place during the northeast monsoon when the EICC flows equatorward carrying low-salinity water along with it (Shetye et al. 1996) and the latter takes place for several months beginning from the peak of summer monsoon. These export pathways are consistent with that seen in climatological data sets and model simulations (Han and McCreary 2001; Jensen 2001; Sengupta et al. 2006). It is quite encouraging to note that the coupled model is able to capture the export pathways correctly.

4 Interannual variability

The interannual SSS variability is examined using monthly anomalies calculated with respect to the 100-year model climatological annual cycle. The standard deviation of the SSS anomalies in CCSM2 (Fig. 7a) exceeds 0.25 over most of the North Indian Ocean. Higher values are seen in the Bay of Bengal with the maximum occurring off the mouths of major rivers. SSS variability is maximum in the northern Bay of Bengal and minimum in the Red Sea and to the south of about 15°S. These model results are in good agreement with the observations that show the standard deviation of SSS in the Indian Ocean in the range of 0.1–0.3 with higher values south of India (Delcorix et al. 2005). Standard deviations higher than 0.5 are also seen off Sumatra in the eastern equatorial Indian Ocean. The interannual variability in the North Indian Ocean is about five times larger than that seen in a coupled model simulation for the Atlantic (Mignot and Frankignoul 2003), but is comparable to that in a model of the western north Atlantic off the mouths of the Amazon and Orinoco rivers (Ferry and Reverdin 2004).

In order to understand the processes that lead to interannual variations in the model, we have calculated standard deviations of the anomalies of each of the terms in the salinity equation. Fresh water input into the ocean (Fig. 7b) has large variability in the Bay of Bengal which is primarily concentrated off the river mouth of Ganga–Brahmhaputra, Godavari–Krishna and Irrawady. Over the rest of the domain, fresh water input variability is rather

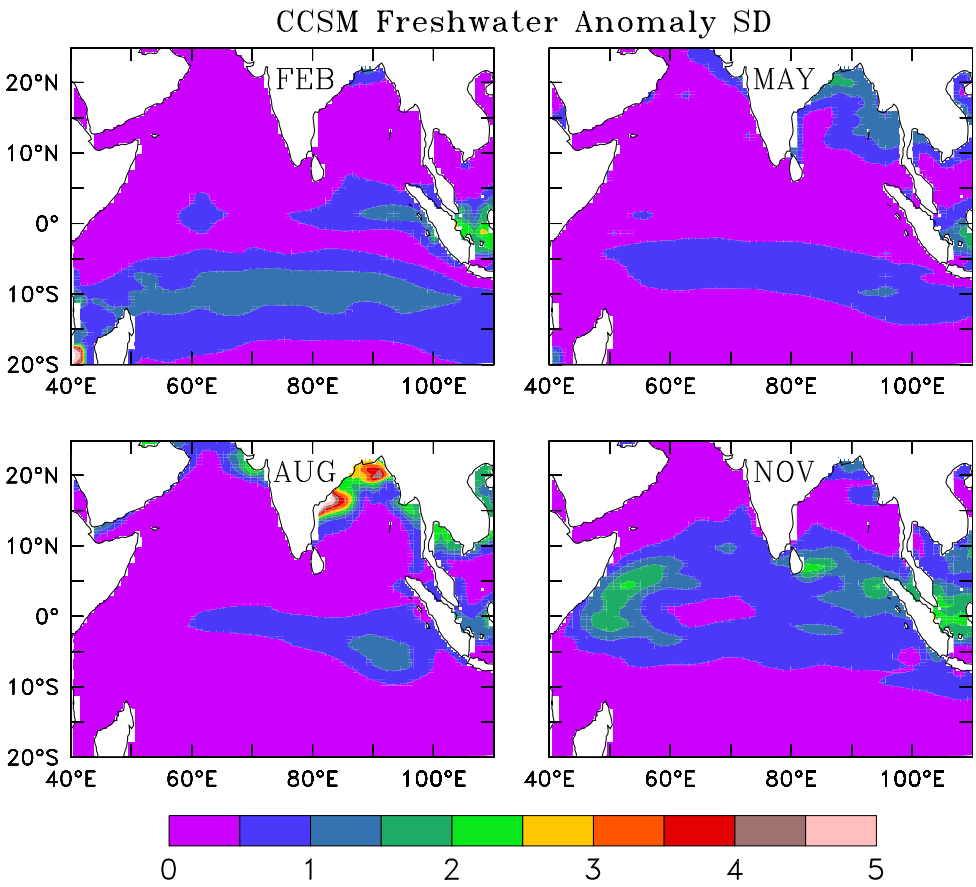

Fig. 9 Same as in Fig. 8 but for the freshwater input term in the salinity equation. Units are 10^{-07} s^{-1}

low. Variability in vertical processes (Fig. 7d) is localized in two regions: one is in the Bay of Bengal along the east coast of India, where a river plume advects equatorward during and the summer monsoon (Shetye et al. 1991, 1996; Vinayachandran et al. 2002a; Vinayachandran and Kurian 2007) and the other is off the coast of Sumatra in the eastern equatorial Indian Ocean. The variability associated with vertical processes is much lower than that of freshwater input and its advection by currents. The standard deviation of horizontal advection anomaly shows largest values among all the three terms on the RHS of Eq. 1. Large advection anomaly standard deviations are seen in the Bay of Bengal and in the eastern equatorial Indian Ocean (Fig. 7c). Advection of low-salinity water from the Bay of Bengal affects the equatorial Indian Ocean to the east of about 70°E. Large advective anomalies indicate that redistribution of freshwater input is an important factor in deciding the spatial structure of interannual SSS variability in the model. Thus, the freshwater input into the Bay of Bengal and its advection determines the interannual variability of SSS in a major part of the north Indian Ocean.

Interannual variability exhibits strong seasonal cycle associated with the monsoons. The monthly anomaly standard deviation ranges between 1 and 2 in the northern Bay of Bengal throughout the year (Fig. 8) but it is less than 1 over most of the North Indian Ocean. In general, the variability is minimum during the pre-monsoon months of April–May over the entire north Indian Ocean. Large seasonal variation in the interannual signal is seen along the east coast of India where the variability is higher during the summer monsoon when the precipitation and river discharge are at their peak. High values are also seen off Sumatra during October–December. The equatorial region is marked by high variability during October–December; two zonal bands on either side of the equator with standard deviation as high as 1 extend westward from the eastern boundary (Fig. 8, November panel). The northern band is stronger and travels westward faster. Both bands extend up to the western boundary during December, with the intensity decreasing westward. This pattern of salinity variability is caused by IOD events (see next section). A similar pattern was noticed by Perigaud et al. (2003) in their interannual salinity simulation using an ocean model forced by observed freshwater forcing. This result is also consistent with the numerical simulation during the IOD event of 1997 (Masson et al. 2004), which showed large negative salinity anomalies to the north of the equator and large positive salinity anomalies to the south. The negative anomalies extend farther westward than the positive anomalies.

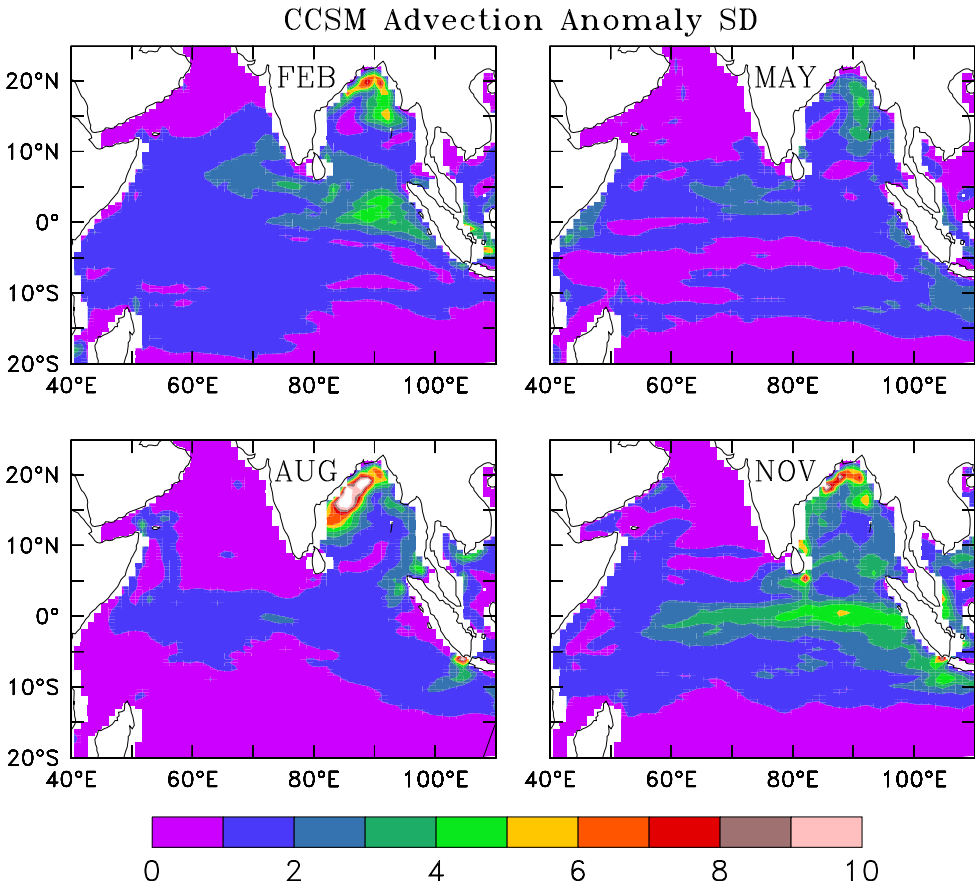

Fig. 10 Same as in Fig. 8 but for the horizontal advection term in the salinity equation. Units are 10^{-07} s^{-1}

Relative roles of net fresh water flux versus advection by ocean currents are examined using monthly standard deviation of anomalies of terms in Eq. 1. The freshwater flux anomaly standard deviation (Fig. 9) suggests that the large interannual standard deviation of salinity in the Bay of Bengal during the summer monsoon is caused by anomalies of $(E - P - R)S/h$. The equatorial Indian Ocean and the southern tropical Indian Ocean show moderate variability in the freshwater forcing during boreal winter. On the other hand, advection anomalies (Fig. 10) contribute throughout the year suggesting that ocean dynamics plays an important role in the persistence of salinity anomalies. Note, for example, that there are large advection anomalies in the Bay of Bengal during February, when the freshwater input does not show a corresponding variability. The flux anomalies lead to some salinity anomaly in the southern tropical Indian Ocean and near the eastern and western boundaries of the EIO during November–December. However, the westward advection of these anomalies appears to have a large contribution to the total salinity anomalies. Influence of vertical processes (Fig. 11) is confined to the east coast of India during the summer monsoon and off the coast of Sumatra during winter; the latter extends westward along the equator in a narrow zonal band.

In summary, the largest interannual variability is seen in the northern Bay of Bengal, where the largest impact of freshwater input associated with the monsoon is felt. Secondary variability is seen off the coast of Sumatra and along the equator. Freshwater input and its advection from the above two source regions determine the interannual variability over a large region in the Indian Ocean.

5 Impact of Indian Ocean Dipole

After the Bay of Bengal, the region with large interannual variability in the model is seen in the eastern equatorial Indian Ocean. It is now well established that there are strong air–sea coupled interannual signals in this region associated with the IOD (Saji et al. 1999; Webster et al. 1999) and ocean dynamics plays a critical role in the evolution of coupled air–sea processes (Murtugudde et al. 1999; Vinayachandran et al. 1999b, 2002b; Vinayachandran and Kurian 2007; Rao et al. 2002; Chang et al. 2006). Large salinity anomalies were present in the eastern equatorial Indian Ocean during the IOD years of 1994 and 1997 and during 1998 (Perigaud et al. 2003; Masson et al. 2004). Salinity anomalies show large standard deviation during November (Fig. 8), when sea surface temperature and sea

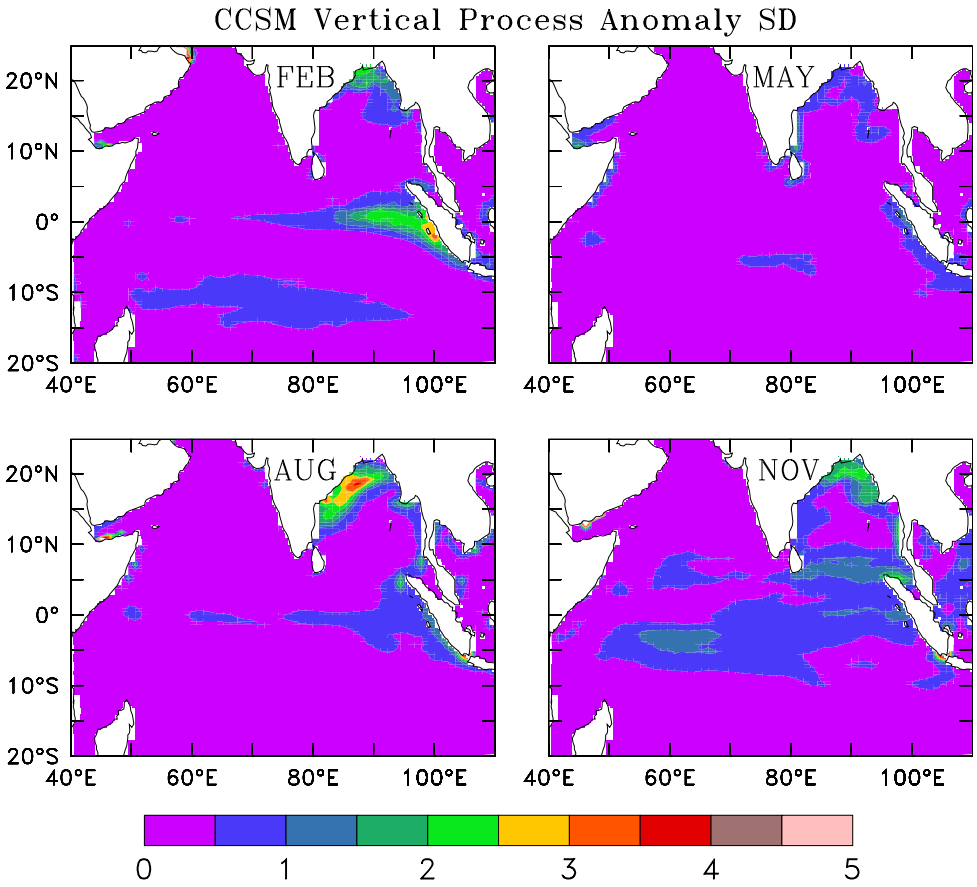

Fig. 11 Same as in Fig. 8 but for the vertical processes term in the salinity equation. Units are 10^{-07} s^{-1}

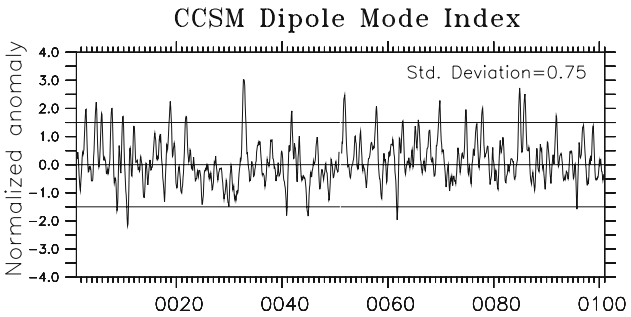

Fig. 12 Dipole Mode Index (DMI) from the model sea surface temperature data set. DMI (Saji et al. 1999) is defined as the difference in SST anomalies between western and eastern Indian Ocean. For the west, average is taken over the box 50°–70°E, 10°S–10°N and for east 90°–100°E, 10°S-Equator. SST anomalies are normalized by their standard deviation shown in the *right corner of the panel*

surface height anomalies associated with the IOD are high. Are the larger variability seen in the CCSM output related to the IOD events in the model? We examine this issue in detail below.

IOD years in the model are identified using the Dipole Mode Index (DMI) as defined by Saji et al. (1999); the DMI is given by the difference in sea surface temperature anomalies between eastern and western equatorial Indian Ocean and is shown in Fig. 12. In this 100-year run, the model simulates several IOD events and the maximum positive DMI occurred during the model year 32. Here we consider the DMI events that lasted for at least 4 months consecutively with the normalized DMI exceeding 1.5 times its standard deviation. There were 20 such events. Composite anomaly maps were prepared for these 20 model IOD years to isolate the influence of these events. Composites were also made for the year before the IOD and the year after it.

Again, there are two regions with high variability: one is in the Bay of Bengal and the other in the eastern equatorial Indian Ocean (Fig. 13). Positive salinity anomalies first appear in the western Bay of Bengal during July of the dipole year and then they spread southward along the east coast of India and eastward in the offshore direction. During January, these anomalies travel around Sri Lanka into the Arabian Sea, along the west coast of India. During October, a band of positive anomaly is seen all across the Bay of Bengal and it is replaced by large negative anomalies in the following January–March period. In the equatorial region, two bands of salinity anomalies—one positive and the other negative—are seen on either side of the equator, both originating from the eastern boundary (Fig. 13, November panel). The negative anomaly band

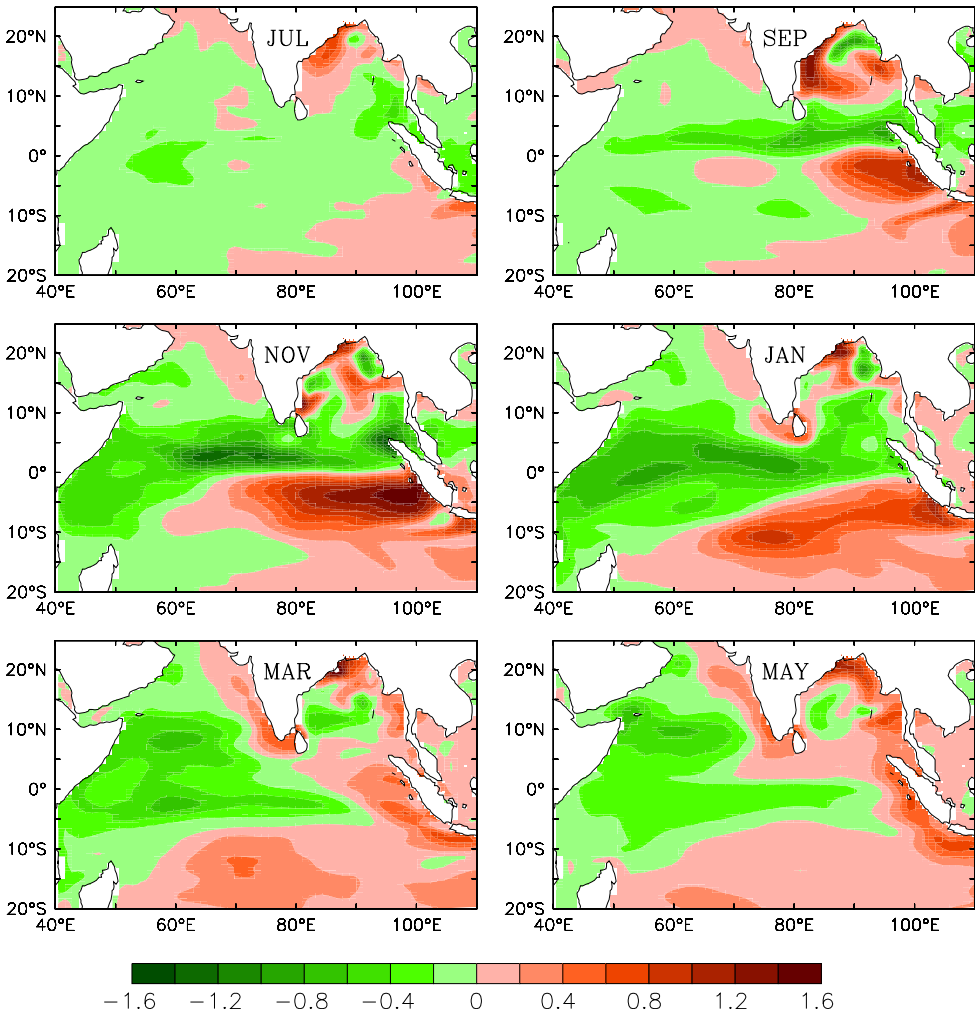

Fig. 13 Bimonthly maps of composite SSS anomaly from the model. Monthly composites are made out of 20 IOD years in CCSM2

appears first, off the northern coast of Sumatra during July and then propagates westward during the summer monsoon. This negative anomaly band extends all across the Indian Ocean by September and remains there for several months. The band of positive anomaly first appears during June–August south of Java, grows further and spreads westward in the following months. This band however, does not penetrate as far westward as the northern band. Although SSS anomalies begin to weaken in January, large negative anomalies exist in the western Indian Ocean and in the south central Indian Ocean till the next summer monsoon.

Masson et al. (2004) used an ocean general circulation model to investigate the salinity effects on the 1997 dipole event. Their salinity simulation showed negative anomalies to the west of Sumatra and positive anomalies over the rest of the equatorial Indian Ocean (between 60° and 90°E, Equator-5°N). The anomaly pattern simulated by the CCSM compares well with this although the negative SSS anomalies in the CCSM extends farther westward suggesting that westward currents are stronger in CCSM. Thompson et al. (2006) examined the salinity anomalies during the IOD years using an ocean general circulation model. The positive salinity anomalies as well as their westward advection in their simulation were weaker than in Masson et al. (2004), probably due to the fact that Thompson et al. (2006) relaxed the model salinity to climatology. The negative anomalies in Thompson et al. (2006), crossed the equator much more to the west than in either Masson et al. (2004) or the present CCSM2 simulation.

In order to find out processes that determine the simulated pattern of SSS anomalies in the coupled model, we have prepared composite maps of all the terms of the salinity equation for the IOD years (Fig. 14). Two bands of SSS anomalies of opposite sign in the equatorial region (Fig. 13, September panel) are located under two bands of precipitation anomalies of opposite sign (Fig. 14b). There is a band of increased precipitation between India and the equator and the low-salinity band is located under this rain belt. Negative rainfall anomalies appear off the coast of Sumatra in August (Fig. 14b), causing positive SSS

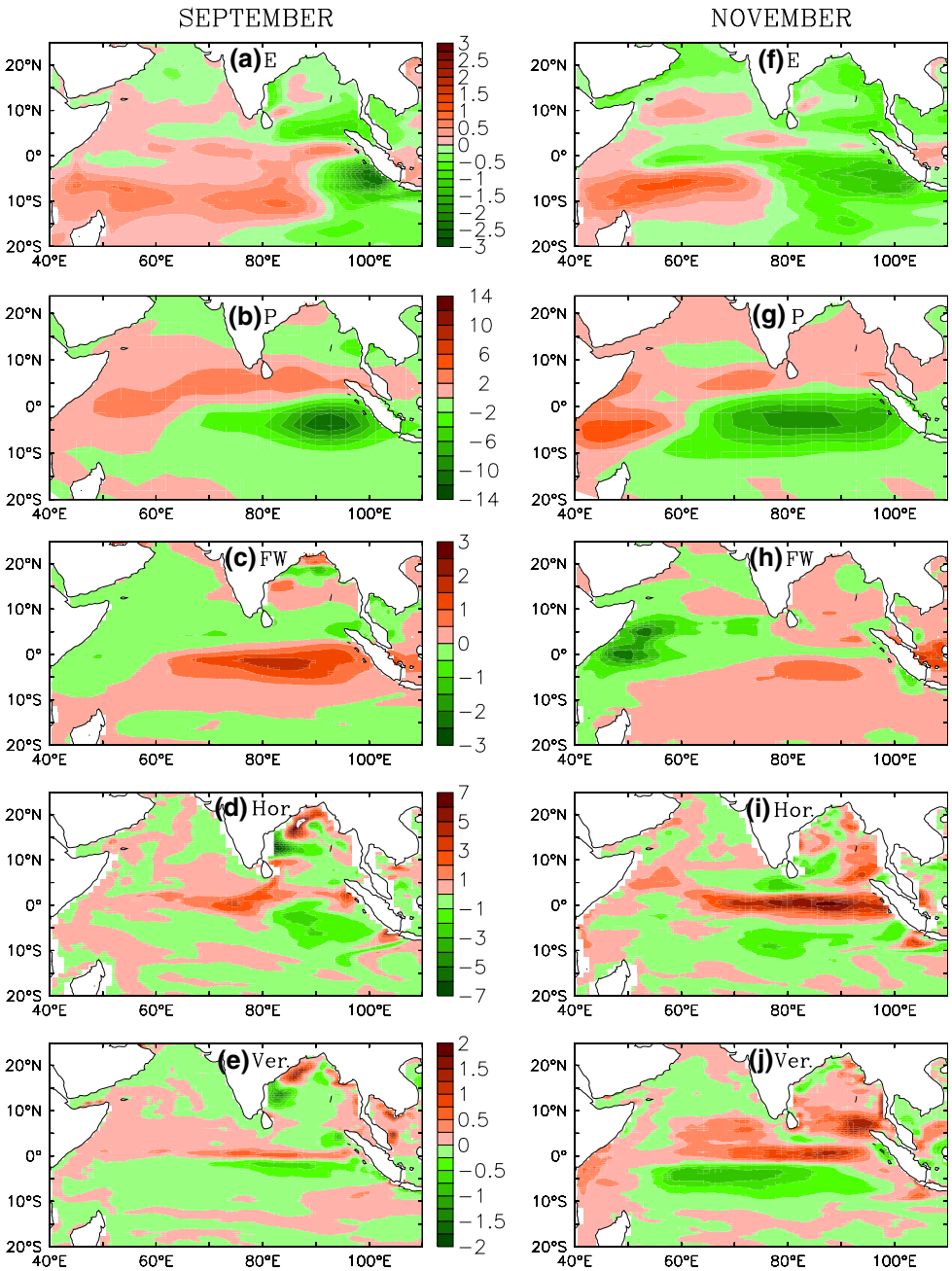

Fig. 14 Composite anomaly maps of for September (*left panels*) and November (*right panels*) for evaporation (**a**, **f**), precipitation (**b**, **g**), freshwater input term (**c**, **h**), horizontal advection term (**d**, **i**) and vertical processes term (**g**, **j**). Units for precipitation and evaporation are mm/day and for the terms of salinity equation it is 10^{-07} s^{-1}

anomalies (Fig. 13) and this negative anomaly patch advects westward in October and November (Fig. 14i). Horizontal advection of positive salinity anomalies are, however, seen in a narrow band confined to the equatorial region, with negative anomalies on either side. Note that the magnitude of contribution from horizontal advection anomaly composites are much higher than that of either fresh water input or vertical processes, particularly near the equator. Oceanic processes, both vertical and horizontal, have more spatial structure than the freshwater input and salinity anomalies. From these maps we find that the atmospheric flux of fresh water into the ocean and its advection by ocean currents determines the simulated composite IOD anomaly patterns.

A very interesting result that has emerged from our analysis is that large salinity anomalies occur in the Indian Ocean during IOD years. Further, anomalies of such magnitude are present only during IOD years. This is illustrated below by considering non-IOD years and El Nino years.

ENSO events in the model were identified using Nino3.4 SST anomalies. Years in which the SSTA exceeded 1.5 standard deviation were defined to be ENSO years and there were eleven such events in the model. Among these,

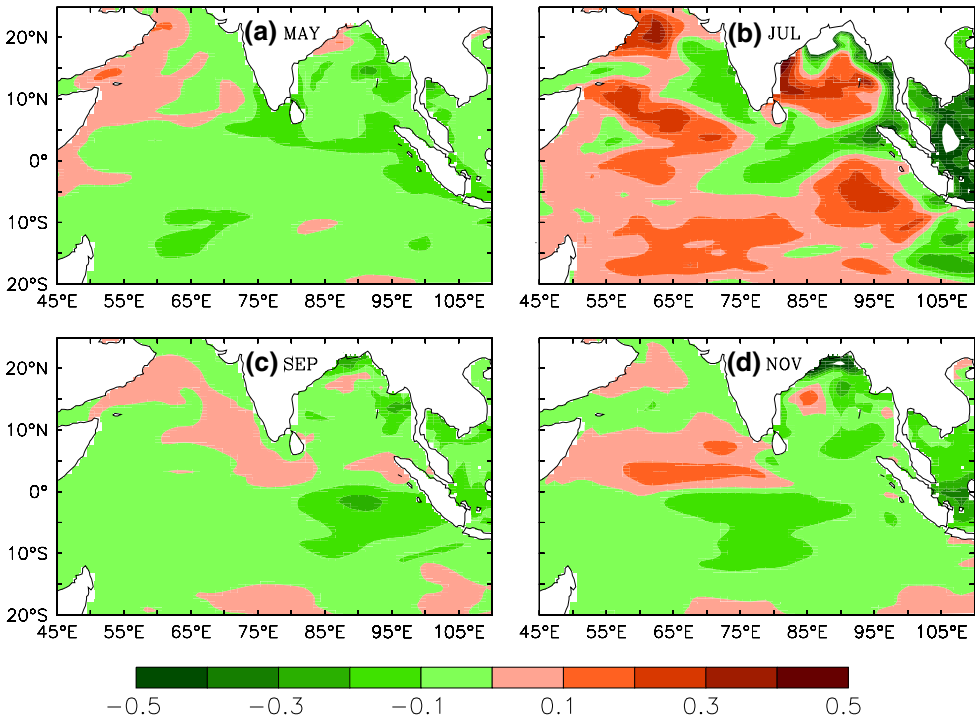

Fig. 15 ENSO composite anomaly maps of SSS for May, July, September and November. Composites are made out of seven El Nino events in the model (see text)

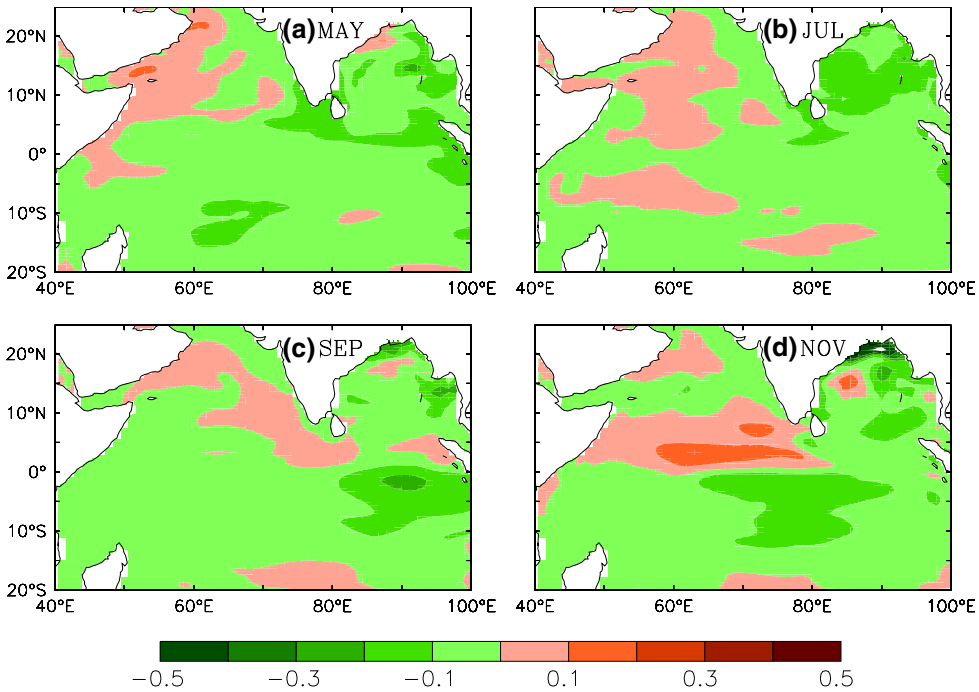

Fig. 16 Residual composite anomaly maps of SSS for m (**a**) May (**b**) July, (**c**) September and (**d**) November. From the 100 years of model output all the IOD years are excluded and the remaining years are used for the composite. In addition, for May and July, the year succeeding an IOD was excluded from the composite

four co-occurred with an IOD event. The remaining seven ENSO events were used for preparing composite maps of pure ENSO events (Fig. 15). During July, positive SSS anomalies are present during El Nino years in the Bay of Bengal, southeastern tropical Indian Ocean and in the Arabian Sea. The coastal regions of the Bay of Bengal show negative salinity anomalies. These anomalies are smaller in magnitude compared to the IOD composite. Moreover, they are short-lived: the anomalies that appear in July do not persist even till September.

The severity of the IOD is manifested in composite anomaly maps for years excluding the IOD years. This is called the residual composite. Figure 16 shows such composites for May, July, September and November. For the case of May and July the year succeeding the IOD year was also excluded from the composite. The residual maps

clearly show that SSS anomalies are much weaker than in the IOD composite (note that the scale of the color bar is different for Figs. 13, 16). Negative anomalies of the order of about 0.4 is seen in the northern Bay of Bengal. The western equatorial Indian Ocean shows anomalies of the order of 0.3 during October–December. Negative anomalies are seen off Sumatra during September in contrast to the positive anomalies seen during IOD years (Fig. 13). In summary, large interannual SSS anomalies exist in the Indian Ocean only during IOD years.

6 Summary and conclusions

The freshwater forcing in the Indian Ocean is characterized by large spatial asymmetry: there is a net freshwater input into the Bay of Bengal and the eastern equatorial Indian Ocean, whereas there is a net loss from the Arabian Sea. Consequently, the salinity in the west is much higher than in the east. A major component of the freshwater input is the large river discharge into the Bay of Bengal. Due to the lack of reliable observations of river discharge, simulation of interannual salinity fields, using ocean models forced by observations, have not been possible. In this paper, we have presented seasonal and interannual variations of Indian Ocean sea surface salinity and their governing processes, from a 100-year simulation using a coupled model (CCSM2).

The seasonal evolution of Indian Ocean salinity distribution in CCSM2 is in good agreement with observations. The export of low-salinity water out of the Bay of Bengal and intrusion of high-salinity water into the bay is reasonably well represented in the model. However, the model SSS is 1–1.5 less than climatology. The main reason for this difference is the overestimation of runoff into the Bay of Bengal, which results from an overestimation of rainfall over Himalayan and Tibetan region, this rainfall draining into the Bay of Bengal through the Brahmaputra and Ganga river systems. On the other hand, the model tends to underestimate the rainfall over the Burmese region, which has short and narrow mountains. It is possible that the poor representation of orography in the atmospheric component of the coupled model is responsible for this deficiency, which might be reduced with an increase in horizontal resolution.

The spatial structure of the seasonal cycle of Indian Ocean SSS is determined by net fresh water input into the ocean (that is, the sum of evaporation, precipitation and runoff) and its redistribution by ocean circulation. Processes that control spatial patterns of salinity are consistent with that obtained from climatological estimates (Rao and Sivakumar 2002). In summer, the fresh water input into the Bay of Bengal and into the eastern equatorial Indian Ocean is the crucial process, whereas during winter the advection by ocean currents becomes the determining factor. Significant vertical exchange of salt and freshwater occurs along the east coast of India and off the coast of Sumatra.

Interannual variations of model salinity are found to be large in the Bay of Bengal (1–2) and in the eastern equatorial Indian Ocean. In the rest of the Indian Ocean, it is, in general, less than 0.5. Most of this variability is caused by the freshwater flux into the Bay of Bengal, into the eastern equatorial Indian Ocean and the advection of these fresh anomalies by ocean currents. The winter-time interannual variations in the equatorial Indian Ocean is marked by two zonal bands along either side of the equator, under the influence of the IOD. The model simulates twenty significant IOD events and large high-salinity anomalies are present off the coast of Sumatra in response to the reduced rainfall in that region. This band extends westward along with the progression of the IOD life cycle. To the north of the high-anomaly region there is a band of low-salinity anomalies that extend all across the Indian Ocean, which is attributed to excess rainfall in this region.

A surprising result from this study is that the Indian Ocean SSS anomalies are high only during the IOD years. A comparison of composite salinity anomaly maps show that the magnitude of salinity anomalies, particularly in the 10°S–10°N band, during the IOD years is about three times larger during IOD years than during non-IOD years and El Nino years.

Acknowledgments This study was funded by the INDOMOD programme of INCOS, Ministry of Earth Science, Government of India. The model simulation was carried out on the PARAM PADMA computer at CDAC, Bangalore. We thank Mr. S. Janakiraman for his help in running the model and Mr. Sharad Kumar Yeri for his help in data analysis. Ferret was used for graphics. We are thankful to Dr. D. Shankar and Dr. S. Iizuka for their comments which helped to improve the paper.

References

Anderson SP, Weller RA, Lukas RB (1996) Surface buoyancy forcing and the mixed layer of the western Pacific warm pool: observations and one-dimensional model results. J Clim 9:3056–3085

Bonan GE, Oleson KW, Vertenstein M, Levis S (2002) The land surface climatology of the Community Land Model coupled to the NCAR Community Climate Model. J Clim 15:3123–3149

Boyer TP, Levitus S (2002) Harmonic analysis of climatological sea surface salinity. J Geophys Res 107. doi:10.1029/2001JC000829

Briegleb BP (1992) Delta-Eddington approximation for solar radiation in the NCAR Community Climate Model. J Geophys Res 97:7603–7612

Chang P, Yamagata T, Schopf P, Behera SK, Carton J, Kessler WS, Meyers G, Qu T, Schott F, Shetye SR, Xie S-P (2006) Climate fluctuations of tropical coupled systems—the role of ocean dynamics. J Clim 19:5122–5174

Conkright ME, Locarnini RA, Garcia HA, O'Brien TD, Boyer TP, Antonov JI, Stephens C (2002) World Ocean Atlas 2001:

objective analyses, data statistics, and figures, CD-ROM Documentation, Technical Report 17, National Oceanic Data Center, Silver Spring, MD
Cooper NS (1988) The effect of salinity on tropical ocean models. J Phys Oceanogr 18:697–707
Donguy J-R, Meyers G (1996) Seasonal variation of sea–surface salinity and temperature in the tropical Indian Ocean. Deep Sea Res I 43:117–138
Delcroix T, McPhaden MJ, Dessier A, Gouriou Y (2005) Time and space scales for sea surface salinity in the tropical oceans. Deep Sea Res Part I 52:787–813
Durand F, Shankar D, Montegut CD, Shenoi SSC, Blanke B, Madec G (2007) Modeling the barrier-layer formation in the southeastern Arabian Sea. J Clim 20:2109–2120
Eriksen C (1979) An equatorial transect of the Indian Ocean. J Mar Res 37:215–232
Ferry N, Reverdin G (2004) Sea surface salinity interannual variability in the western tropical Atlantic: an ocean general circulation model study. J Geophys Res 109. doi:10.1029/2003JC002122
Godfrey JS, Bradley EF, Coppin PA, Pender LF, McDougall TJ, Schula EW, Helmond I (1999) Measurements of upper ocean heat and freshwater budget near a drifting buoy in the equatorial Indian Ocean. J Geophys Res 104:13269–13302
Gualdi S, Guilyardi E, Navarra A, Masina S, Delecluse P (2003) The interannual variability in the tropical Indian Ocean as simulated by a coupled GCM. Clim Dyn 20:567–582
Han W, McCreary JP, Anderson DLT, Mariano AJ (1999) Dynamics of the eastern equatorial surface jets in the equatorial Indian Ocean. J Phys Oceanogr 29:2191–2209
Han W, McCreary JP (2001) Modeling salinity distribution in the Indian Ocean. J Geophys Res 106:859–877
Han W, Webster PJ (2002) Forcing mechanisms of sea level interannual variability in the Bay of Bengal. J Geophys Res 32:216–239
Howden SD, Murtugudde R (2001) Effects of river inputs into the Bay of Bengal. J Geophys Res 106:19825–19843
Iizuka S, Matsuura T, Yamagata T (2000) The Indian Ocean SST dipole simulated in a coupled general circulation model. Geophys Res Lett 27:3369–3372
Janakiraman S, Nanjundiah RS, Vinayachandran PN (2005) Simulations of the Indian summer monsoon with a coupled ocean-atmosphere model on PARAM-PADMA. Curr Sci 89:1555–1562
Jensen TG (2001) Arabian Sea and Bay of Bengal exchange of salt and tracers in an ocean model. Geophys Res Lett 28:3967–3970
Jensen TG (2003) Cross-equatorial pathways of salt and tracers from the northern Indian Ocean: modelling results. Deep Sea Res Part I 50:2111–2127
Josey E, Kent CE, Taylor P (1999) New insights into the ocean heat budget closure problem from analysis of the SOC air–sea flux climatology. J Climate 12:2856–2880
Kiehl JT, Gent PR (2004) The community climate system model, Version 2. J Climate 17:3666–3676
Kurian J, Vinayachandran PN (2006) Formation mechanisms of temperature inversions in the southeastern Arabian Sea. Geophys Res Lett 33. doi:10.1029/2006GL027280
Kurian J, Vinayachandran PN (2007) Mechanisms of formation of the Arabian Sea mini warm pool in a high-resolution Ocean General Circulation Model. J Geophys Res 112. doi:10.129/2006JC003631
Large WG, McWilliams JC, Doney SC (1994) Oceanic vertical mixing: a review and a model with a nonlocal boundary layer parameterization. Rev Geophys 32:363–403
Lau NC, Nath MJ (2003) Atmosphere–ocean variations in the Indo-Pacific sector during ENSO episodes. J Clim 16:3–20
Lukas R, Lindstrom E (1991) The mixed layer of the western equatorial Pacific Ocean. J Geophys Res 96:3343–3357
Masson S, Delecluse P, Boulanger J-P, Menkes C (2002) A model study of the seasonal variability and formation mechanisms of the barrier layer in the eastern equatorial Indian Ocean. J Geophys Res 107. doi:10.1029/2001JC000832
Masson S, Boulanger J-P, Menkes C, Delecluse P, Yamagata T (2004) Impact of salinity on the 1997 Indian Ocean dipole event in a numerical experiment, J Geophys Res 109. doi:10.1029/2003JC001807
McCreary JP, Kundu PK, Molinary R (1993) A numerical investigation of dynamics, thermodynamics and mixed-layer processes in the Indian Ocean. Prog Oceanogr 31:181–244
Mignot J, Frankignoul C (2003) On the interannual variability of sea surface salinity in the Atlantic. Clim Dyn 20:555–565
Miller JR (1976) The salinity effect in a mixed layer ocean model. J Phys Oceanogr 6:29–35
Murtugudde R, Busalacchi AJ (1998) Salinity effects in a tropical ocean model. J Geophys Res 103:3283–3300
Murty VSN, Sarma YVB, Rao DP, Murty CS (1992) Water characteristics, mixing and circulation in the Bay of Bengal during southwest monsoon. J Mar Res 50:207–228
Nanjundiah RS, Vidyunmala V and Srinivasan J (2005) On the difference in the seasonal cycle of rainfall over India in the Community Climate System Model (CCSM2) and Community Atmospheric Model (CAM2). Geophys Res Lett 32. doi:10.1029/2005GL024278
Phillips HE, Wijffels SE, Feng M (2005) Interannual variability in the freshwater content of the Indonesian–Australian Basin. Geophys Res Lett 32. doi:10.1029/2004GL021755
Perigaud C, McCreary JP, Zhang KQ (2003) Impact of interannual rainfall anomalies on Indian Ocean salinity and temperature variability. J Geophys Res 108. doi:10.1029/2002JC001699
Rao RR, Sivakumar R (2002) Seasonal variability of sea surface salinity and salt budget of the mixed layer of the north Indian Ocean. J Geophys Res 107. Doi:10.1029/2001JC00907
Rao SA, Behera SK, Masumoto Y, Yamagata T (2002) Interannual variability in the subsurface Indian Ocean with special emphasis on the Indian Ocean dipole. Deep Sea Res Part II 49:1549–1572
Saji NH, Goswami BN, Vinayachandran PN, Yamagata T (1999) A dipole model in the tropical Indian Ocean. Nature 401:360–363
Sengupta D, Raj GNB, Shenoi SSC (2006) Surface freshwater from Bay of Bengal runoff and Indonesian throughflow in the tropical Indian Ocean. Geophys Res Lett 33. doi:10.1029/2006GL027573
Schott F, McCreary JP (2001) The monsoon circulation in the North Indian Ocean. Progr Oceanogr 51:1–123
Shankar D, Vinayachandran PN, Unnikrishnan AS (2002) The monsoon currents in the north Indian Ocean. Prog Oceanogr 52:63–120
Shankar D, Gopalakrishna VV, Shenoi SSC, Durand F, Shetye SR, Rajan CK, Johnson Z, Araligidad N, Michael GS (2004) Observational evidences for westward propagation of temperature inversions in the southeastern Arabian Sea. Geophys Res Lett 31. doi:10.1029/2004GL019652
Shenoi SSC, Shetye SR, Gouveia AD, Michael GS (1993) Salinity extrema in the Arabian Sea. In: Ittekkot V, Nair RR (eds) Monsoon biogeochemistry. Uni Hamburg, Germany, pp 37–49
Shenoi SSC, Shankar D, Michael GS, Kurian J, Varma KK, Ramesh Kumar MR, Almeida Unnikrishnan AS, Fernandes W, Barreto N, Gnanaseelan C, Mathew R, Praju KV, Mahale V (2005) Hydrography and water masses in the southeastern Arabian Sea during March–June 2003. J Earth Sys Sci 114:475–491
Shetye SR, Shenoi SSC, Gouveia AD, Michael GS, Sundar D, Nampoothiri G (1991) Wind-driven coastal upwelling along the western boundary of the Bay of Bengal during the southwest monsoon. Cont Shelf Res 11:1397–1408
Shetye SR, Gouveia AD, Shankar D, Shenoi SSC, Vinayachandran PN, Sundar D, Michael GS, Nampoothiri G (1996) Hydrography

and circulation in the western Bay of Bengal during the northeast monsoon. J Geophys Res 101:14011–14025

Smith RD, Gent PR (2002) Reference Manual for the Parallel Ocean Program (POP): Ocean Component of the Community Climate System Model (CCSM–2). Available at http://www.ccsm.ucar.edu/models/ccsm2.0.1/pop/

Smith RD, McWillimas JC (2003) Anisotropic horizontal viscosity for ocean models. Ocean Model 5:129–156

Smagorinsky J (1963) General circulation experiments with the primitive equations. Mon Weather Rev 91:99–164

Sprintall J, Tomczak M (1992) Evidence of the barrier layer in the surface layer of the tropics. J Geophys Res 97:7305–7316

Thompson B, Ganaseelan C, Salvekar PS (2006) Variability in the Indian Ocean circulation and salinity and its impact on SST anomalies during dipole events. J Mar Res 64:853–880

Vinayachandran PN, Kurian J (2007) Hydrographic observations and model simulation of the Bay of Bengal freshwater plume. Deep Sea Res Part I 54:471–486

Vinayachandran PN, Masumoto Y, Mikawa T, Yamagata T (1999a) Intrusion of the southwest monsoon current into the Bay of Bengal. J Geophys Res 104:11077–11085

Vinayachandran PN, Saji NH, Yamagata T (1999b) Response of the equatorial Indian Ocean to an unusual wind event during 1994. Geophys Res Lett 26:1613–1615

Vinayachandran PN, Murty VSN, Ramesh Babu V (2002) Observation of barrier layer formation in the Bay of Bengal during summer monsoon, J Geophys Res 107. doi:10.1029/2001JC000831

Vinayachandran PN, Iizuka S, Yamagata T (2002b) Indian Ocean dipole mode events in an ocean general circulation model. Deep Sea Res II 49:1573–1596

Vinayachandran PN, Kagimoto T, Masumoto Y, Chauhan P, Nayak SR, Yamagata T (2005) Bifurcation of the East India Coastal Current east of Sri Lanka. Geophys Res Lett 32. doi:10.1029/2005GL022864

Vorosmarty CJ, Fekete B, Tucker BA (1996) River Discharge Database, Version 1.0 (RivDIS v1.0), vols 0–6. A contribution to IHP-V Theme 1, Technical Documents in Hydrology Series, Technical Report. United Nations Educational, Scientific and Cultural Organisation, Paris

Webster PJ, Moore AM, Loschnigg JP, Leben RR (1999) Coupled ocean–atmosphere dynamics in the Indian Ocean during 1997–1998. Nature 401:356–360

Xie P, Arkin PA (1998) Global monthly precipitation estimates from satellite-observed outgoing longwave radiation. J Clim 11:137–164

Xie S-P, Xu H, Saji NH, Wang Y (2006) Role of narrow mountains in organization of Asian summer monsoon. J Clim 19:3420–3429

Yaremchuk M, Yu Z and McCreary JP (2005) River discharge into the Bay of Bengal in an inverse ocean model. Geophys Res Lett 32. doi:10.1029/2005GL023750

Zhang GJ, McFarlane NA (1995) Sensitivity of climate simulations to the parameterization of cumulus convection in the Canadian Climate Centre general circulation model. Atmosphere-Ocean 33:407–446